Microelectronic Engineering 106 (2013) 43–47

Contents lists available at SciVerse ScienceDirect

Microelectronic Engineering

journal homepage: www.elsevier.com/locate/mee

Series resistance study of Schottky diodes developed on 4H-SiC wafers using a contact of titanium or molybdenum

K. Shili [a,*], M. Ben Karoui [a], R. Gharbi [a], M. Abdelkrim [a], M. Fathallah [a], S. Ferrero [b]

[a] *Laboratoire des Semi-conducteurs et Dispositifs Electroniques. C3S, Ecole Supérieure des Sciences et Techniques de Tunis, University of Tunis, 05 Av. Taha Hussein, 1008 Montfleury, Tunis, Tunisia*

[b] *Politecnico di Torino, c.so Duca Degli Abruzzi, 10129 Torino, Italy*

ARTICLE INFO

Article history:
Received 12 July 2012
Received in revised form 21 December 2012
Accepted 7 February 2013
Available online 26 February 2013

Keywords:
Schottky diode
Series resistance
Ti or Mo/4H-SiC
Electrical model

ABSTRACT

We have studied and compared two types of Schottky diodes prepared by the evaporation of molybdenum (Mo) and titanium (Ti) on a 4H-SiC semiconductor. The electrical characteristics of these diodes are analyzed based on the standard thermionic emission model. The main electrical parameters including the series resistance R_s, the ideality factor n and the barrier height Φ_B are extracted from current–voltage–temperature (I–V–T) measurements. In the Ti/4H-SiC structure, the series resistance increases from 1.51 mΩ cm^2 to 27.68 mΩ cm^2 when the temperature is varied from 70 K to 450 K. In contrast, the series resistance does not exceed a 6.17 mΩ cm^2 at 450 K in the Mo/4H-SiC Schottky diode. We have decomposed the series resistance into three components. The deduced static and dynamic parameters were used to define an electrical model. The switching behavior of the equivalent circuit indicates a reverse recovery time (Trr) of 1.412 ns for Ti/4H-SiC and 3.27 ns for Mo/4H-SiC.

1. Introduction

Silicon carbide has attracted a great deal of attention in recent years because of its potential applications in a wide array of components. Silicon carbide is an appropriate material for high temperature, high frequency and high power electronic devices, due to its wide band gap (3–3.2 eV), high breakdown field (>2×10^6 V cm^{-1}), and high thermal conductivity (5 W cm^{-1} K^{-1}) [1].

Recent technological improvements have led to the use of the polytype 4H to fabricate efficient devices such as Schottky barrier diodes (SBDs) and junction field effect transistors (JFETs) [2].

In general, the overall performance of an SBD is affected by several factors such as the surface characteristics of the semiconductor, the metal work function and the properties of the metal/semiconductor interface [3,4]. To study the performances of 4H-SiC SBDs, we have compared the electrical behaviors of diodes with molybdenum (Mo) and titanium (Ti) Schottky contacts over a range of temperatures.

2. Experimental details

Schottky diodes were developed on 4H-SiC wafers and prepared with a metal-oxide overlap for electric field termination. A silicon dioxide thin film was grown on the epilayer by standard 13.56 MHz PECVD (plasma enhanced chemical vapor deposition). The reactive gases were CO, SiH and H. The radio frequency power was maintained at 30 W, the substrate temperature was kept at 450 °C, and the pressure was set to 0.6 Torr. An additional thermal treatment was carried out in a hot furnace at 1000 °C in an oxygen atmosphere to improve the quality of the silicon dioxide films.

A Schottky barrier was formed on the 4H-SiC epilayer by thermal evaporation under vacuum. This was performed using two different metals Ti or Mo with or without thermal annealing in a controlled atmosphere as described in Table 1. The active area (A) of the device was 1 mm^2. The samples were processed by standard lithographic processes to create a metal-oxide guard ring aimed at avoiding electric field crowding at the Schottky contacts. Ohmic contacts were formed on the back of the wafer by a triple evaporation of titanium, nickel and silver for all the samples [5]. Fig. 1 provides the details of the layers in the Ti and Mo Schottky diodes.

The electrical properties were extracted from I–V analysis, performed in the cryogenic system from 70 K to 450 K by a Keithly model 6517A electrometer/high resistance meter. The dynamic properties were studied using a DC–DC converter circuit. An external variable power supply was used with a model chopper from Techno System Company with a variable frequency and with pulsed width modulation (PWM) techniques.

The capacitance of the device versus frequency and the voltage bias were measured using a HP 4274A (100 Hz–100 kHz) LCR meter and a HP 4192 (1 kHz–1 MHz) impedance analyzer.

* Corresponding author.
E-mail address: rached.gharbi@esstt.rnu.tn (K. Shili).

0167-9317/$ - see front matter © 2013 Elsevier B.V. All rights reserved.
http://dx.doi.org/10.1016/j.mee.2013.02.043

Table 1
Electrical parameters of Mo and Ti Schottky contacts.

Parameters	n	R_s [mΩ cm^2]	Φ_B [eV]	I_R @ −600 V [μA]
Ti no ann.	1.02	9.6	0.83	1600
Ti/4H-SiC ann.400 °C	1.14	7.2	1.01	1000
Mo no ann.	1.09	2.227	0.96	1700
Mo/4H-SiC ann. 400 °C	1.07	5.49	0.91	100
Mo/4H-SiC ann. 600 °C	1.05	7.12	1.10	120

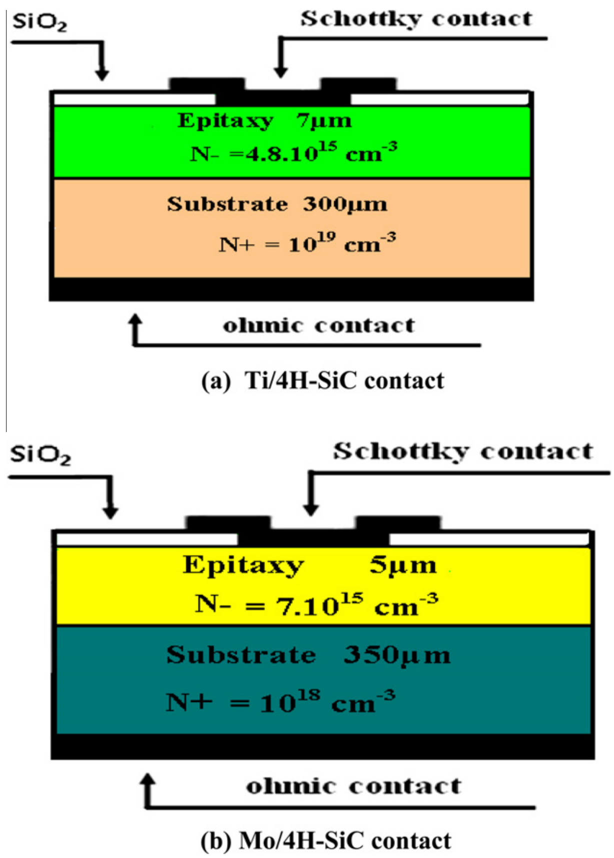

Fig. 1. Structure of studied Schottky diodes (a) Ti/4H-SiC contact and (b) Mo/4H-SiC contact.

3. Results and discussion

The total current density J across the junction can be related to the thermionic emission theory of Schottky, expressed as:

$$J = \left[A^*T^2 \exp\left(-\frac{q\Phi_B}{kT}\right)\right]\left[\exp\left(\frac{qV}{nkT}\right) - 1\right] \quad (1)$$

A^* is the Richardson's constant, Φ_B is the effective Schottky barrier height (SBH), n is the ideality factor, q is the elementary charge and k is Boltzmann's constant. For 4H-SiC, the published value of $A^* = 145$ A/cm^2 K^2 [6].

The saturation current $I_s = J_s A$ can be extrapolated from the J-axis intercept of a log (J) versus V plot. The barrier height Φ_B can be directly evaluated from Eq. (2):

$$\Phi_B = \frac{kT}{q}\left(\frac{AA^*T^2}{I_S}\right) \quad (2)$$

The ideality factor n can be obtained from the slope of the log (J) versus V curve. Usually, n takes into account any deviation from ideal SBD behavior. Furthermore, the series resistance (R_s) of the Schottky diode can be evaluated from the slope of the linear portion of the J–V curve.

Fig. 2 shows the variation of J–V for two types of Schottky diodes at 300 K, the Mo diode and the Ti diode annealed at 400 °C. We extract the previously defined electrical parameters from J–V characteristics. Between 0.2 V and 0.6 V, we can determine the ideality factor n. At 300 K, the saturation current I_s was estimated at 10^{-14} A for Ti/4H-SiC and 10^{-12} A for Mo/4H-SiC. When the direct voltage is greater than 0.6 V, we can determine the series resistance R_s by calculating the reverse slope of the curve in this region.

The diodes with Ti and Mo Schottky contacts have been prepared at different annealing temperatures: 400 °C for the Ti contact and 600 °C for the Mo diode. Table 1 reports the parameters extracted for the devices, including the Schottky barrier height or SBH (Φ_B), the ideality factor (n) and the series resistance (R_s).

The Schottky diode based on Ti/4H-SiC shows a breakdown reverse voltage (V_{BD} obtained at a reverse current of 1 mA) of 600 V for the device annealed at 400 °C, and 100 V for the structure obtained without annealing. These results indicate that the quality of the Schottky contact depends on annealing. When the diode with Ti Schottky contact was annealed at 400 °C, the SBH increases from 0.83 eV to 1.01 eV. On the contrary, the SBH of the diode with Mo contact decreases from 1.04 eV to 0.91 eV when it is annealed at 400 °C, and increases to 1.10 eV when the annealing temperature is increased to 600 °C. In both types of diodes, the reverse current I_R at −600 V decreases as the annealing temperature is increased, and this decrease is more notable in the Mo/4H-SiC device (Table 1).

The ideality factor n of the Ti/4H-SiC increases from 1.02 to 1.14 after annealing at 400 °C. In Mo/4H-SiC contacts, the values of n were relatively unaffected by the thermal treatment (Table 1). While the annealing affects the series resistance of the two Schottky contacts: for Ti, R_s decreases from 9.6 mΩ cm^2 without annealing to 7.2 mΩ cm^2 after annealing at 400 °C. For Mo, which has smaller series resistances than Ti/4H-SiC, R_s varies from 2.227 mΩ cm^2 without annealing to 7.12 mΩ cm^2 when the junction is annealed at 600 °C.

To study and understand the contributions of different regions to the series resistance, we consider the following expression of the current density J in forward conduction:

$$J = A^*T^2 \exp^{\frac{qV_F}{nkT}} \exp^{-\frac{q\Phi_B}{kT}} \quad (3)$$

At the low voltage bias, the threshold potential V_F can be expressed as:

$$V_F = \frac{nkT}{q} \cdot \ln\left(\frac{J}{A^*T^2}\right) + n\Phi_B \quad (4)$$

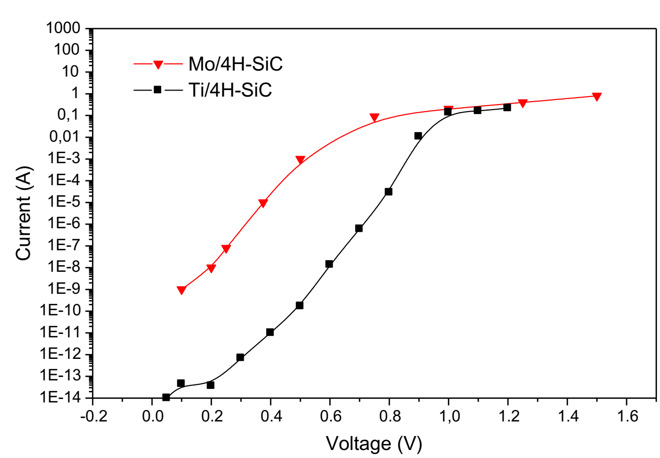

Fig. 2. Forward characteristics of Mo and Ti SBDs, Tann. = 400 °C.

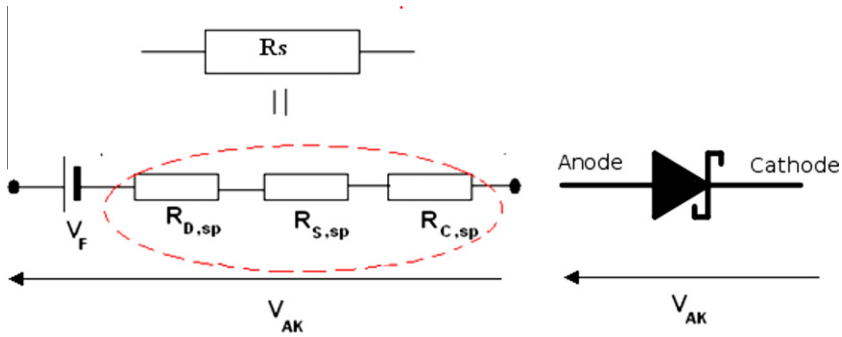

Fig. 3. Equivalent circuit of Schottky diode in direct conduction.

For a high voltage bias, we can write:

$$V_s = R_s J = \left(\frac{W_D}{qN_D\mu_D} + \frac{W_S}{qN_S\mu_S} + R_C\right) \cdot J \tag{5}$$

where W_D, N_D, and μ_D represent the width, density of doping and electron mobility of the drift region in the epitaxial layer, respectively, and W_S, N_S and μ_S represent the same parameters in the substrate layer. R_C represents the ohmic contact. The forward voltage V_{AK} is the combination of the two effects:

$$V_{AK} = V_F + V_S$$
$$= \frac{nkT}{q} \cdot \ln\left(\frac{I}{AA^*T^2}\right) + n\Phi_B + \left(\frac{W_D}{qN_D\mu_D} + \frac{W_S}{qN_S\mu_S} + R_C\right) \cdot \frac{I}{A} \tag{6}$$

This expression quite accurately describes the direct characteristics of the diode, and appears in most publications on this topic [7,3,8].

As the diode under study here includes three layers, namely, the epitaxial, substrate and ohmic contact layers, we have adopted the equivalent model of the diode presented in Fig. 3.

The drift region is necessary to avoid exceeding the maximum allowable electric field of the semiconductor and thus increasing the voltage that must be supported. To ensure the desired breakdown voltage, a junction of minimal length must be built in the lightly doped region. The thickness of the drift region is reduced to a minimum value to optimize the direct resistance. The extension of this space charge region in the junction is limited, and the electric field is then not zero at the end of the lightly doped region.

The total resistance R_s (Ω cm^2) is calculated using the doping level N, thickness W and electron mobility μ of the epitaxial and substrate layers. Friedrichs et al. [9] mentioned that the drift layer should be doped to the highest possible degree. The specific drift region resistance $R_{D,sp}$ can be described by Eq. (9).

$$W_D = \frac{2V_R}{E_{\lim}} \tag{7}$$

$$N_D = \frac{\varepsilon E_{\lim}^2}{2qV_R} \tag{8}$$

$$R_{D,sp} = \frac{W_D}{qN_D} * \frac{1}{\mu_n(T)} = \frac{4V_R^2}{\varepsilon E_{\lim}^3} * \frac{1}{\mu_n(T)} \tag{9}$$

where E_{lim} = 2.10^6 V/cm is the limited electrical field, V_R is the reverse voltage, ε = 10 is the permittivity and μ_n is the electron mobility in cm^2/V s.

The specific substrate resistance $R_{s,sp}$ is given by:

$$R_{S,sp} = \frac{W_S}{qN_S} * \frac{1}{\mu_n(T)} \tag{10}$$

Table 2
Parameters used for the model of the 4H-SiC Schottky diode at T = 300 K.

Parameters	Symbol	Value for Ti/ 4H-SiC	Value for Mo/ 4H-SiC	Unit
Schottky barrier height	Φ_B	1.1	0.91	eV
Substrate widh	W_S	300	350	μm
Substrate doping	N_S	10^{19}	10^{18}	cm^{-3}
Drift widh	W_D	7	5	μm
Drift doping	N_D	4.8$*10^{15}$	7$*10^{15}$	cm^{-3}
Electron mobility	μ_n(T) (Eq. 11)			cm^2/V s

The specific ohmic contact resistance to n-type SiC is important as mentioned by La Via et al. [10]. We considered that $R_{c,sp}$ = 10^{-5} - Ω cm^2 for Ti and $R_{c,sp} \approx 1*10^{-4}$ Ω cm^2 for Mo. Increasing the temperature and time of annealing can significantly decrease the resulting contact resistance [11].

Thermal effects are important for all power semiconductor devices. The electrical behavior of the junction barrier Schottky (JBS) rectifier depends strongly on the operating temperature of the device. For the SiC JBS rectifier, we have assumed that all donor atoms in the drift region are ionized at room temperature. The electron mobility given by Eq. (11) depends on the temperature, the donor concentration and the electrical field [12].

$$\mu_n(T) = \mu_n^{\min} + \frac{\mu_n^{delta}}{1 + \left(\frac{N_D+N_A}{N_n^{\mu}}\right)^{\gamma_n}} \cdot \left(\frac{T}{300K}\right)^{\alpha_n} \tag{11}$$

where N_D is the concentration of ionized donors and N_A is the concentration of ionized acceptors.

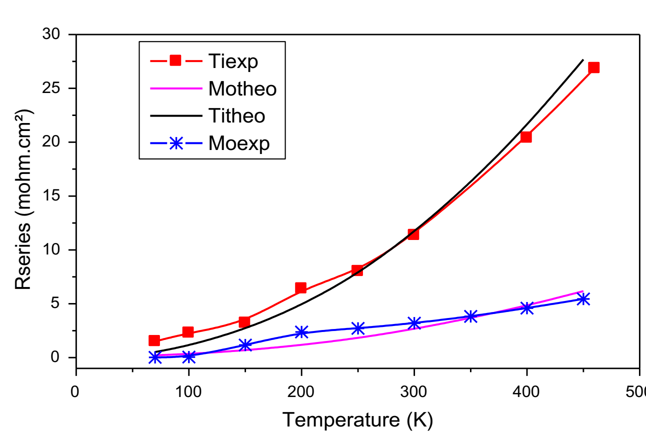

Fig. 4. Variation of series resistance R_s as function of temperature for Ti and Mo theoretical and experimental curves.

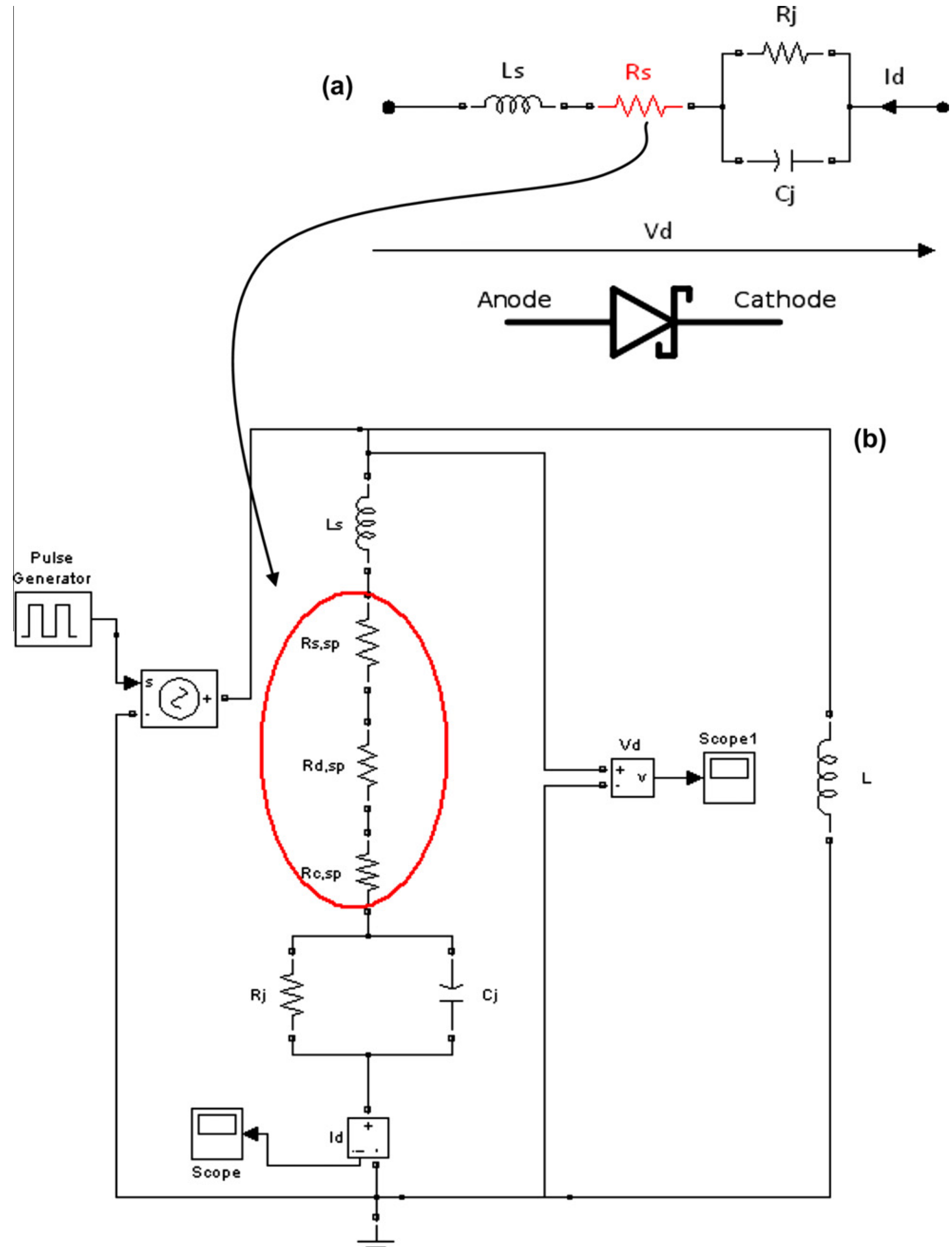

Fig. 5. (a) Equivalent dynamic circuit of Schottky diode and (b) Considered equivalent circuit used as a model of the diode with Simulink.

The following temperature-dependent parameters have been determined [12]:

$$\mu_n^{\min} = 0\ \text{cm}^2/\text{V s}, \mu_n^{delta} = 947\ \text{cm}^2/\text{V s}, N_n^{\mu} = 1.9410^{17}\ \text{cm}^{-3}, \gamma_n = 0.61 \text{and} \alpha_n = -2, 15.$$

We have used the parameters given in Table 2 and the appropriate equations to calculate the series resistances. Fig. 4 shows the experimental and simulated variation of the series resistance R_s of (Ti/4H-SiC) and (Mo/4H-SiC) versus temperature. We observe that the series resistance in Ti/4H-SiC increases from 0.5182 mΩ cm^2 at 70 K to 27.68 mΩ cm^2 at 450 K. In the Mo/4H-SiC device, the series resistance increases to a lesser degree, from 0.212 mΩ cm^2 at 70 K to 6.17 mΩ cm^2 at 450 K. The series resistance is more stable to changes of the temperature in Mo/4H-SiC than in Ti/4H-SiC.

In spite of the annealing improves the quality of Schottky contacts in the two types of diode, the evolution of series resistance versus temperature is more significant in Ti/4H-SiC and depends on the quality of metal/semiconductor contact. There are a number of physical reasons to which the quality of metal–semiconductor contact can be ascribed; the main disadvantage of Ti/SiC is the rough interface with the substrate [10]. The interface roughness has an effect on the specific contact resistance. However, this roughness can be minimized by careful cleaning of the substrate before titanium deposition. In order to obtain the minimum specific contact resistance the backside ohmic contact has been annealed at very high temperature.

The carrier transport mechanism at the metal/SiC interface and which has been studied and discussed in the literature [13] contributes in the formation of this interface, on the other hand the difference in the crystal symmetry of the metal with respect to the semiconductor or variation in the orientation at the

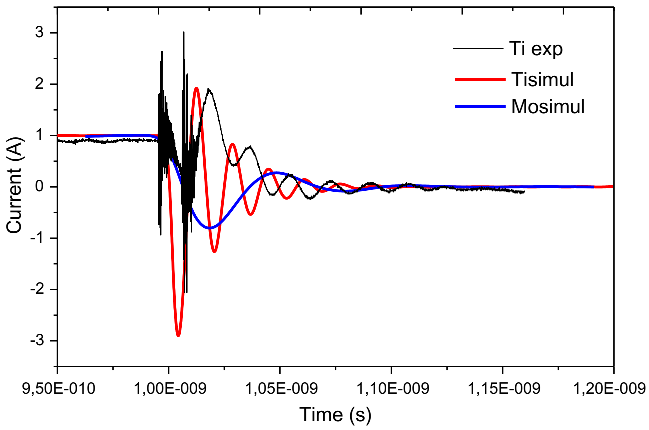

Fig. 6. Current waves for Ti/4H-SiC and Mo/4H-SiC measured and simulated under conditions (V_F = 40 V, I_F = 1A).

metal–semiconductor interface, due to localized faceting of the interface, the mixture of different metallic phases with different SBH's and contaminations are probably other features which can lead to variation of series resistance and SBH inhomogeneities [14]. Many authors have investigated the properties of the metal/SiC interface to obtain reproducible and stable rectifier devices [15–17].

After considering the series resistance of the diode, we integrate the values obtained from the equivalent model of the diode to determine its dynamic behavior and the influence of this series resistance on the switching phenomenon. The electrical model of the dynamic behavior of the diode was developed using Matlab-Simulink is shown in Fig. 5 and was previously studied in Ti/4H-SiC [18]. We used the measured capacitances Cj = 500 pF for titanium and 800 pF for molybdenum at 300 K. The series resistance R_s was deduced from the I–V characteristics of the device, and L_s represents the inductance of the pin and packaging process. Some previous publications [19] have shown that parasitic components depend on the cell geometry and proposed a comprehensive model taking the effect of transistors in commutation into account.

We integrated the previous results of the Simulink simulation using the equivalent dynamic circuit of the Schottky diode. Fig. 6 shows the variations of the experimental current waves for Ti/4H-SiC and simulated waves for Mo/4H-SiC and Ti/4H-SiC under the conditions of V_F = 40 V and I_F = 1 A.

The parameters describing the switching transients at the opening of the diode are the maximum reverse current I_{RM} and the reverse recovery time Trr, providing information about the speed of the diode. The waveforms of the currents show that the maximum amplitude of the oscillation is greater in Ti/4H-SiC (−2.88 A) than in Mo/4H-SiC (−0.8 A). Fig. 6 shows a reverse recovery time Trr of approximately 1.412 ns for Ti/4H-SiC compared to 3.27 ns for Mo/4H-SiC. Weaker oscillations were observed for Mo/4H-SiC, and the measured period of oscillation in Ti/4H-SiC diode is fourteen times the period in Mo/4H-SiC one. These differences are due to the parameters of the diodes, in particular the junction capacitance Cj [20].

4. Conclusion

The Ti/4H-SiC and Mo/4H-SiC Schottky diodes are studied and compared. The Schottky contacts were prepared with and without annealing in the temperature range of 400–600 °C. The variation of series resistance versus temperature in Ti/4H-SiC structure is more important compared to the Mo/4H-SiC one, SiC due to the interface between metal and semiconductor material. The annealing improves the ideality factor and SBH who are more stable in Mo/4H-SiC diode. In reverse polarization, the saturation current is higher in Mo/4H-SiC than in Ti/4H-SiC, providing evidence that the leakage current is more important. The Ti/4H-SiC exhibits more rapid changes in dynamic behavior, although the maximum amplitude of the weakened oscillations in the current wave is greater than one for Mo/4H-SiC Schottky diode.

References

[1] A. Itoh, H. Matsunami, Phys. Status Solidi (a) 162 (1997) 389.
[2] J.B. Casady, R.W. Johnson, Solid-State Electron. 39 (1996) 1409–1422.
[3] A. Itoh, T. Kimoto, H. Matsunami, IEEE Electron Device Lett. 16 (1995) 280.
[4] M. Furno, F. Bonani, G. Ghione, S. Ferrero, S. Porro, P. Mandracci, L. Scaltrito, D. Perrone, G. Richieri, L. Merlin, Mater. Sci. Forum 941 (2005) 483–485.
[5] L. Scaltrito, G. Fanchini, S. Porro, M. Cocuzza, Diamond Relat. Mater. 12 (2003) 1224–1226.
[6] M.E. Levinshtein, S.L. Rumyantsev, M.S. Shur, Properties of Advanced Semiconductor Materials, John Wiley Inc., New York, 2001.
[7] S.M. Sze, in: Modern Semiconductor Device Physic, John Wiley & Sons, 1997, ISBN 0-471-15237-4.
[8] K.P. Schoen, J.M. Woodall, J.A. Cooper, M.R. Melloch, IEEE Trans. Electron Devices 45 (1998) 1595–1604.
[9] P. Friedrichs, D. Stephani, Microelectron. Eng. 83 (2006) 181–184.
[10] F. La Via, F. Roccaforte, A. Makhtari, V. Raineri, P. Musumeci, L. Calcagno, Microelectron. Eng. 60 (2002) 269–282.
[11] J. Crofton, L.M. Porter, J.R. Williams, Status Solidi (b) 202 (1997) 581.
[12] M. Bakowski, U. Gustafsson, U. Lindefelt, Phys. Status Solidi (a) 162 (1997) 421.
[13] A. Frazzetto, F. Giannazzo, R. Lo Nigro, V. Raineri, F. Roccaforte, J. Phys. D: Appl. Phys. 7 (25) (2011).
[14] M. Ben Karoui, R. Gharbi, N. Alzaied, M. Fathallah, E. Tresso, L. Scaltrito, S. Ferrero, Solid-State Electron. 52 (2008) 1232–1236.
[15] F. Roccaforte, J. Phys. D: Appl. Phys. 43 (2010) 22.
[16] M. Badila, G. Brezeanu, J. Millan, P. Godignon, V. Banu, Diamond Relat. Mater. 11 (2002) 1258–1262.
[17] Lingqin Huang, Bingbing Liu, Qiaozhi Zhu, Suhua Chen, Mingchao Gao, Fuwen Qin, Appl. Phys. Lett. 100 (2012) 263503.
[18] K. Shili, M. Ben Karoui, R. Gharbi, M. Abdelkrim, M. Fathallah, S. Ferrero, Dynamic behavior of Ti/4H-SiC Schottky diodes, in: 13th IEEE Mediterrean Electrotechnical Conference MELECON, 2012, pp. 626–629.
[19] M. Besacier, M. Coyaud, J.L.Schanen, J. Roudet, B.Rivet, Hybrid Si-Sic fast switching cell modelling and characterisation including parasitic environment description by PEEC method, 33rd Power Electronics Specialists conference, 2002, pp. 1753–1757.
[20] Tsuyoshi Funaki, Tsunenobu Kimoto, Takashi Hikihara, IEEE Trans. Power Electron. 23 (5) (2008) 12–52.